Available online at www.sciencedirect.com
SCIENCE DIRECT®
Journal of Power Sources 124 (2003) 241–245
JOURNAL OF POWER SOURCES
www.elsevier.com/locate/jpowsour

Short communication

$CaSi_2$ as an anode for lithium-ion batteries

J. Wolfenstine*

Army Research Laboratory, AMSRL-SE-DC, 2800 Powder Mill Road, Adelphi, MD 20783-1197, USA

Received 2 June 2003; accepted 12 June 2003

Abstract

$CaSi_2$ was investigated as a potential anode material for use in lithium-ion batteries. The capacity was investigated as a function of particle size. The capacity at 50 cycles of the as-sieved $CaSi_2$ material (25–30 μm) is about 150 and 220 mAh/g for the ball-milled (1–3 μm) material, suggesting that neither will make a good replacement anode for graphite. A majority of the $CaSi_2$ capacity is associated with Si and not Ca, which is in agreement with predicted behavior. A comparison of the capacity fade of $CaSi_2$ with other silicides suggests that to minimize capacity fade, it is better to have in materials that under go decomposition during Li insertion, a high modulus and/or low ductility matrix than a low modulus and/or high ductility matrix.
Published by Elsevier B.V.

Keywords: Anode; Li-ion batteries; Capacity; Elastic modulus; Silicide

1. Introduction

Recently, there has been interest in the use of intermetallic silicides as replacement anodes for graphite in Li-ion batteries [1–9]. One such silicide that has received considerable attention is Mg_2Si [1,2,5,6,8]. Mg_2Si prepared by conventional melting (particle sizes less than 70 μm) exhibited an initial specific capacity of 1370 mAh/g which decreased to about 100 mAh/g after 10 cycles when the alloy was cycled to a lower limit of about 5 mV [5]. For the case of Mg_2Si prepared by mechanical alloying (mean particle size of about 30 μm) the alloy exhibited an initial specific capacity of 830 mAh/g, which rapidly decreased, to 100 mAh/g after five cycles when cycled in the voltage range 5 mV–0.65 V [6]. Changing the voltage limits (50–225 mV) for the mechanical alloyed material increased the discharge capacity to a value of about 100 mAh/g, which was approximately constant for 25 cycles. For both the as-melted and mechanical alloyed Mg_2Si it was suggested at low potentials that it decomposed into binary Li–Si and Li–Mg alloys [5,6].

Another intermetallic silicide that has not received any attention as a potential anode for use in Li-ion batteries is $CaSi_2$. There are two reasons why $CaSi_2$ could be a potential anode. The first reason is its promise of high reversible Li capacity. For example, $CaSi_2$ upon lithium insertion at low potentials based on the predicted Ca–Si–Li room temperature ternary phase diagram should decompose into binary Li–Si and Li–Ca alloys as follows [3]:

$$10.8\,Li + CaSi_2 \rightarrow Li_2Ca + 2\,Li_{4.4}Si \quad (1)$$

The predicted reversible capacity associated with the above reaction would be 3015 mAh/g of $CaSi_2$. This is eight times the theoretical value for graphite (372 mAh/g [1]). The second reason is the promise of low capacity fade compared to other silicides. In the case of NiSi and FeSi, which also form $Li_{4.4}Si$ dispersed within a metal matrix (i.e. Ni or Fe) upon Li insertion, rapid capacity fade was exhibited [9]. These silicides have high melting temperature matrices, which in general results in low ductility materials [10–13], which may account for the rapid capacity fade observed. In contrast, as a result of its low melting point, T_m, [$T_m = 503$ K, 230 °C] it may be expected that Li_2Ca could provide a highly ductile matrix at room temperature for the $Li_{4.4}Si$ alloy to expand and contract within and thus, $CaSi_2$ may exhibit low capacity fade compared to other silicides.

It is the purpose of this paper to investigate the possibility (i.e. capacity and capacity fade) of $CaSi_2$ as a potential anode for use in Li-ion batteries as a function of particle size and compare the results to other silicides that have been considered as anodes for use in Li-ion batteries.

2. Experimental

$CaSi_2$ powders were obtained from Alpha Aesar. The powders were crushed, ground and sieved to less than 44 μm.

* Tel.: +1-301-394-0317; fax: +1-301-394-0273.
E-mail address: jwolfenstine@arl.army.mil (J. Wolfenstine).

0378-7753/$ – see front matter. Published by Elsevier B.V.
doi:10.1016/S0378-7753(03)00731-6

To check on the effect of particle size on capacity and capacity fade some of the sieved powders were placed in a hardened steel jar with a ball to powder weight ratio of 5:1 under an atmosphere having an oxygen concentration and moisture level of less than 1 ppm. These powders were then milled using a high-energy ball-mill (Spex-8000) for 20 h. In addition, to determine how much of the capacity was associated with Ca, Ca powders were obtained form Alpha Aesar and were ground and crushed and sieved to less than 44 μm under an atmosphere having an oxygen concentration and moisture level of less than 1 ppm. The $CaSi_2$ powders were characterized by X-ray diffraction (XRD), scanning electron microscopy (SEM) and Brunauer–Emmett–Teller (BET).

The cycle life of the $CaSi_2$, ball-milled $CaSi_2$ and Ca powders were evaluated in half-cells at room temperature. $CaSi_2$ and ball-milled $CaSi_2$ positive electrodes were prepared by mixing 85 wt.% active material, 5 wt.% carbon and 10 wt.% polyvinylidene fluoride dissolved in *N*-methylpyrrolidinone. The mixture was coated onto a Cu substrate. The electrodes were dried under vacuum. For the case of Ca positive electrodes, these were prepared by cold-pressing the powders with no binder or conductive agent onto a Ni-grid. Metallic lithium was used as the negative electrode. Cells were constructed by placing the positive electrode, Celegard 2300 separator and lithium foil pressed onto a Ni grid between two 1/8 in. thick polypropylene blocks. The cells were placed in foil laminate pouches and 4 g of a 1 M $LiPF_6$:ethlylene carbonate (EC)/diethyl carbonate (DEC) (1:1 (v/v)) solution was added. The cells were cycled at a constant current density of 20 $\mu A/cm^2$ between 0.005 and 1.50 V.

3. Results and discussion

The X-ray diffraction patterns of the as-sieved and ball-milled $CaSi_2$ powders are shown in Fig. 1. From Fig. 1, it can be seen that the as-sieved material exhibits very sharp and narrow diffraction peaks indicating a highly crystalline material with a particle size in the micron range. In contrast, the diffraction peaks in the ball-milled material are highly reduced in intensity and broad compared to the as-sieved material. These results suggest a less crystalline material with a smaller particle size for the ball-milled $CaSi_2$ compared to the as-sieved material. SEM analysis revealed that the particle size of the as-sieved material was between 25 and 30 μm. SEM analysis of the ball-milled material revealed a particle size between 1 and 3 μm. BET analysis assuming spherical particles [14] yielded a particle size of about 1 μm for the balled-milled material. The average crystallite size calculated using the Scherrrer formula [15] was 1 μm for the balled-milled material. Hence, it can be concluded that the particle size of the ball-milled material (1–2 μm) is about 18 times smaller than that for the as-sieved material (25–30 μm). In addition, there is a large broad hump in the balled-milled pattern at low diffraction angles, suggesting some percentage of the balled-milled material is amorphous. The X-ray diffraction pattern for the Ca powders (25–30 μm) revealed only sharp and narrow diffraction peaks for single-phase Ca.

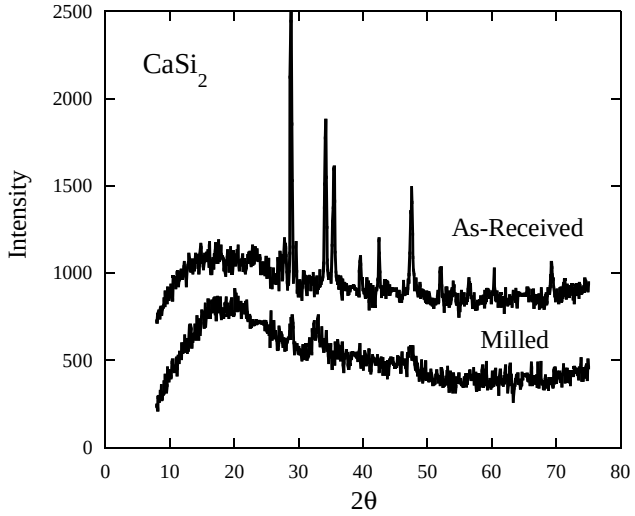

Fig. 1. X-ray diffraction patterns of the as-sieved and ball-milled $CaSi_2$ powers.

A typical discharge–charge cycle, after the first cycle, for the as-sieved $CaSi_2$ powders is shown in Fig. 2. From Fig. 2, it can be observed that during discharging (Li addition) that no Li insertion takes until the voltage is below about 0.3 V. This is in good agreement with values for crystalline Mg_2Si, which are close to 0.3 V [1,5,6]. In the voltage window between 0.3 and 0.005 V, three distinct regions exist, with a plateau between about 0.16–0.07 V. The three regions are in agreement with behavior predicted by the room temperature ternary phase diagram for Ca–Si–Li [3]. A typical discharge–charge cycle, after the first cycle, for the

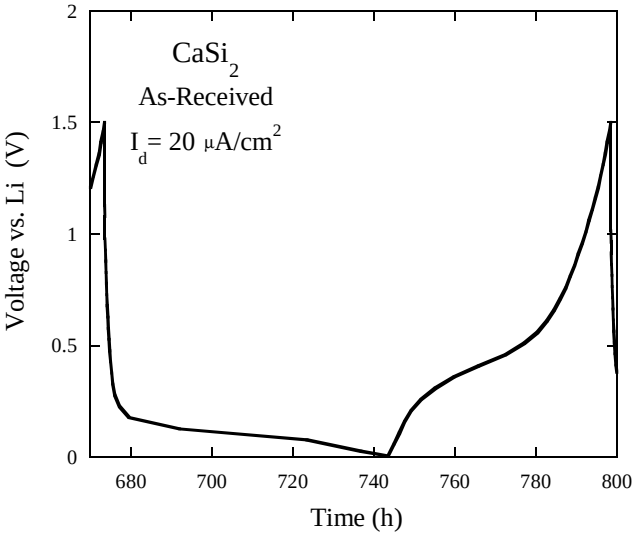

Fig. 2. Typical discharge curve for the as-sieved $CaSi_2$ cycled between 0.005 and 1.5 V.

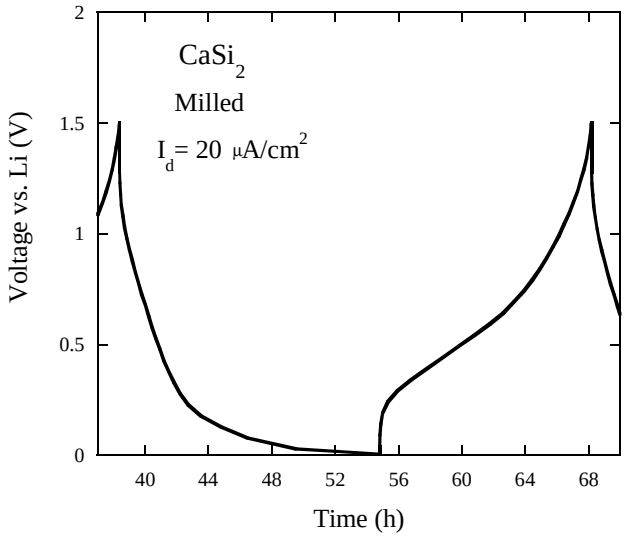

Fig. 3. Typical discharge curve for the ball-milled $CaSi_2$ cycled between 0.005 and 1.5 V.

ball-milled $CaSi_2$ powders is shown in Fig. 3. From Fig. 3, no plateaus or knees are observed in the discharge curve of the ball-milled $CaSi_2$ material, only a sloping curve, with a gradual change in voltage with composition is exhibited. A sloping curve is typical for an amorphous material [16–18] and confirms the amorphous nature of the ball-milled material shown by the X-ray diffraction plot in Fig. 1. The pure Ca powder showed several distinct regions with insertion beginning at about 0.3 V.

The specific capacity of the as-sieved and ball-milled $CaSi_2$ powders versus cycle number is plotted in Fig. 4. Also included in Fig. 4 is data for the Ca powders. From Fig. 4, several important points are noted. Firstly, the Li capacity associated with the Ca powders is very low in magnitude compared to graphite and exhibits rapid capacity fade. For example, at 50 cycles, the capacity of Ca is about 10 mAh/g compared to practical values of between 300 and 350 mAh/g for graphite [1]. The capacity drops from 400 to 12 mAh/g after 10 cycles. From these results, it is anticipated that even with the addition of a binder that the capacity of the Ca powders will still be very low compared to graphite. Secondly, the reversible Li capacity of the $CaSi_2$ powders is associated mainly with Si and not Ca. This is in agreement with what is predicted by Eq. (1). From Eq. (1), out of the total Li capacity associated with the decomposition of $CaSi_2$ the predicted Li percentage capacity for Ca (Li_2Ca) is 18.5% and for Si ($Li_{4.4}Si$) 81.5%. From Fig. 4, it is observed that the Li capacity ratio of Ca to $CaSi_2$ of similar particle size (25–30 μm) is about 3%, suggesting that 97% of the capacity of $CaSi_2$ is associated with Si. This result confirms that a majority of the capacity is associated with Si, in agreement with Eq. (1). However, it is higher than expected (97% versus 81%). A potential explanation for the higher capacity is a result of the fact that there is excess Si in the $CaSi_2$ phase and/or slow kinetics associated with formation of the Li_2Ca phase at room temperature. The third important point from Fig. 4 is that the capacity of the ball-milled $CaSi_2$ is greater than that for the as-sieved $CaSi_2$. For example, at the 50th cycle, the capacity of the ball-milled material is 220 mAh/g compared to 150 mAh/g for the as-sieved material. This is a result of its smaller particle size and/or amorphous nature. This is in agreement with behavior observed in oxides and metal alloys, which show enhanced capacity as the particle size is reduced or as the material becomes more amorphous [18–22]. Fourthly, the capacity of the both the as-sieved and ball-milled $CaSi_2$ powders is low in magnitude compared to graphite and exhibits rapid capacity. For example, at the 50th cycle, the capacity of the as-sieved $CaSi_2$ material is about 150 and 220 mAh/g for the ball-milled material, compared to practical values of between 300 and 350 mAh/g for graphite [1]. Thus, suggesting that neither the as-sieved or the ball-milled $CaSi_2$ materials will make a good replacement anode for graphite in Li-ion batteries.

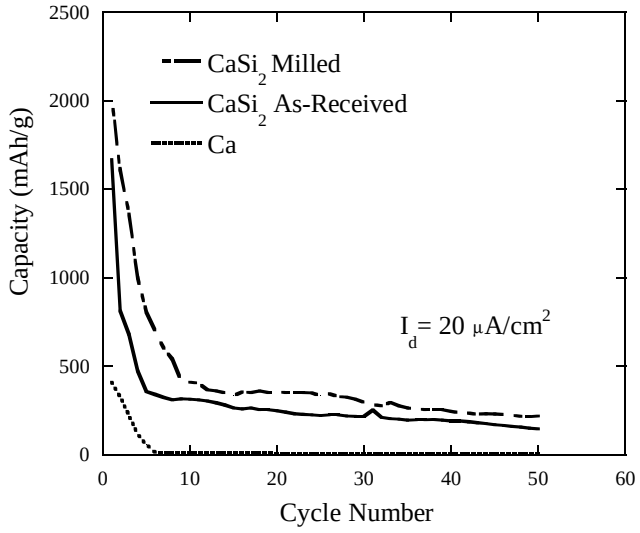

Fig. 4. Discharge capacity for the as-sieved $CaSi_2$, ball-milled $CaSi_2$ and Ca materials. The cells were cycled between 0.005 and 1.5 V.

The capacity at the 10th cycle is 400 mAh/g for the ball-milled $CaSi_2$ and 310 mAh/g for the as-sieved $CaSi_2$. The capacity at the 10th cycle ranges from 100 to 200 mAh/g for Mg_2Si [5,6], 720 mAh/g for FeSi [9] and 920 mAh/g for NiSi [9]. The capacity values for the $CaSi_2$ materials at the 10th cycle are within the range of what has been exhibited by other silicides. The observed capacity for the silicides at the 10th cycle is low compared to theoretical values (i.e. ≈3000 mAh/g for $CaSi_2$ and ≈1400 mAh/g for FeSi). The low values of the actual capacity compared to theoretical values at a small number of cycles represents rapid capacity fade and is a result of the large volume change(s) that occur upon reaction with Li. The volume change(s) cause mechanical stress, which causes particles to loose contact with the electrode, leading to the decrease in capacity. It is of interest to speculate why the Mg–Si and Ca–Si alloys exhibit lower capacity at given cycle (i.e. faster capacity fade) compared to the Fe–Si and Ni–Si alloys. The same trend

exits for the Mg–Si, Ca–Si, Fe–Si and Ni–Si alloys when the capacity is normalized per gram of Si. There are several potential explanations. One possible reason may have to do with a difference in the stress generated do the volume change during Li insertion. If all the Mg–Si, Ca–Si, Fe–Si and Ni–Si alloys undergo decomposition with Li insertion it would be expected that they all form the same Li–Si alloys with last being $Li_{4.4}Si$, and hence, all will undergo the same volume change and generate the same value of stress. Thus, in a first approximation volume change cannot explain the difference in capacity between the silicide alloys. Another potential reason could be related to a difference in particle size. However, based on the results of Fig. 4, it is unlikely that this could explain the large difference observed between the Mg–Si, Ca–Si, Fe–Si and Ni–Si alloys. A more likely reason has to do with the mechanical properties of the matrix. In this case, it could be related to the elastic properties (i.e. elastic modulus) and/or the plastic properties (i.e. ductility) of the matrix. There is not sufficient enough elastic modulus and ductility data available for the four silicide alloys to make a detailed comparison to determine the exact relationship between the mechanical properties and capacity fade and to separate the effects of modulus from ductility on capacity fade. However, a rough comparison can be made between the mechanical properties and capacity fade since, it is known that the elastic modulus in a first approximation scales with the melting point of a material [11–13] while ductility scales inversely with melting temperature [11–13]. For the case of the Ca–Li and Mg–Li systems, the matrix is composed of Li_2Ca and an Mg–Li alloy, respectively. For the case of the Ni–Si and Fe–Si systems, the matrix is Ni and Fe, respectively. The melting point of: (1) Ni is 1726 K (1453 °C); (2) Fe is 1809 K (1536 °C); and (3) Li_2Ca is 503 K (230 °C). For the case of the Mg–Li alloy since, no composition [5,6] is given an exact melting temperature (solidus temperature) cannot be specified. However, based on the shape of the Mg–Li phase diagram [23] it is estimated that the solidus temperature for the Mg–Li alloy will fall between that for Mg, 922 K (649 °C), and that for Li, 454 K (181 °C). Consequently, the matrices for the Mg–Si and Ca–Si alloys upon Li insertion exhibit much lower melting temperatures compared to the Fe–Si and Ni–Si alloys. Hence, it is expected Ni and Fe have a higher elastic modulus and exhibit lower ductility than the Li_2Ca and an Mg–Li alloys. The elastic modulus at room temperature for Ni and Fe is 200 and 211 GPa, respectively [10]. No data is available for the elastic modulus of Li_2Ca. Since the melting point of the Li_2Ca alloy is 503 K (230 °C) compared to a melting point of 1115 K (842 °C) for pure Ca, it would be a good first estimation to suggest that the maximum modulus for Li_2Ca is on the order of that for Ca, 20 GPa. Based on the shape of the Mg–Li phase diagram [23], it is estimated that the modulus for the Mg–Li alloy will fall between that for Mg, 45 GPa, and that for Li, 4.9 GPa. Thus, the matrices for the Mg–Si and Ca–Si alloys upon Li insertion exhibit much lower values for the elastic modulus (<50 GPa) compared to the Fe–Si and Ni–Si alloys (≈200 GPa). The capacity fade of the low modulus materials was much faster than that for the high modulus materials. A matrix with a higher elastic modulus may provide a larger residual compressive stress than a matrix with a lower elastic modulus, which could relieve the tensile stresses generated as a result of the Li reaction with Si, and thus, lower capacity fade would be expected in the material with the higher elastic modulus matrix. For the case of ductility, sufficient data does not exist for Mg–Si and Ca–Si alloys to make the same comparison as was done for the case of the elastic modulus. However, based on the melting point prediction, it is expected that Ni and Fe will exhibit lower ductility compared to Li_2Ca and the Mg–Li alloy. The capacity fade of the materials with the lower ductility was much less than that for the more ductile materials. These results are in agreement with those of Nishio and Furukawa [24] who showed that for Li–Al electrodes that more than a factor of three improvement in cycle life was obtained when the matrix was hardened (i.e. matrix became less ductile). In addition, the results of this study are in excellent agreement with recent results of Wang et al. [25] who suggested based on electrochemical impedance spectroscopy of Li-alloys contained within a matrix that the matrix should have low ductility to maximize cycle life. A matrix with a low ductility modulus may provide a larger residual compressive stress than a matrix with a greater ductility, which could relieve the tensile stresses generated as a result of the Li reaction with Si, and thus, lower capacity fade would be expected in the material with the lower ductile matrix. At present, it is not possible to separate which of the two effects; modulus or ductility has a greater influence on capacity fade.

4. Conclusions

The capacity of $CaSi_2$ as a function of particle size was investigated and compared to other silicides that have been considered as anodes for use in Li-ion batteries. It was observed that a majority of the $CaSi_2$ capacity is associated with Si and not Ca, which is in agreement with predicted behavior. The capacity of ball-milled $CaSi_2$ is greater than that for as-sieved $CaSi_2$. This is a result of its smaller particle size and/or amorphous nature. The capacity of both the as-sieved and ball-milled $CaSi_2$ powders is low in magnitude compared to graphite. For example, at 50 cycles, the capacity of the as-sieved $CaSi_2$ is about 150 and 220 mAh/g for ball-milled $CaSi_2$. These results suggest that neither the as-sieved nor the ball-milled $CaSi_2$ materials will make a good replacement anode for graphite. A comparison of the capacity fade of $CaSi_2$ with other silicides suggests that to minimize capacity fade it is better to have in materials that under go decomposition during Li insertion, a high modulus and/or low ductility matrix than a low modulus and/or high ductility matrix.

Acknowledgements

The author would like to acknowledge support of the Army Research Laboratory. Thanks are due to Mr. Steven Campos for his technical assistance.

References

[1] C.-K. Huang, S. Suarampudi, A.I. Attia, G. Halpert, US Patent 5,294,503 (1994).
[2] R.A. Huggins, Solid State Ionics 152–153 (2002) 61.
[3] A. Anani, R.A. Huggins, J. Power Sources 38 (1992) 351.
[4] A. Anani, R.A. Huggins, J. Power Sources 38 (1992) 363.
[5] H. Kim, J. Choi, H.-J. Sohn, T. Kang, J. Electrochem. Soc. 146 (1999) 4401.
[6] G.A. Roberts, E.J. Cairns, J.A. Reimers, J. Power Sources 110 (2002) 424.
[7] W.J. Weydanz, M. Wohlfahrt-Mehrens, R.A. Huggins, J. Power Sources 81–82 (1999) 237.
[8] T. Moriga, K. Watanabe, D. Tsuji, S. Massaki, L. Nakabayahsi, J. Solid State Chem. 153 (2000) 386.
[9] G.X. Wang, L. Sun, D.H. Bradhurst, S. Zhong, S.X. Dou, H.K. Liu, J. Power Sources 88 (2000) 278.
[10] W.D. Callister, Materials Science and Engineering, Wiley, New York, 1997.
[11] M.W. Barsum, Fundamentals of Ceramics, McGraw-Hill, New York, 1997.
[12] M.F. Ashby, D.R.H. Jones, Engineering Materials, Pergamon Press, Oxford, 1986.
[13] C.R. Barrett, W.D. Nix, A.S. Tetelman, The Principles of Engineering Materials, Prentice-Hall, New York, 1973.
[14] L. Kavan, M. Gratzel, Electrochem. Solid State Lett. 5 (2002) A39.
[15] B.D. Cullity, Elements of X-Ray Diffraction, Addison-Wesley, Reading, MA, 1978.
[16] H. Jung, M. Park, Y.-G. Yoon, G.-B. Kim, S.-K. Joo, J. Power Sources 115 (2003) 346.
[17] L. Fang, B.V.R. Chowdrai, J. Power Sources 97–98 (2001) 181.
[18] G. Pistoia, M. Pasquali, G. Wang, L. Li, J. Electrochem. Soc. 137 (1990) 2365.
[19] H. Li, X. Huang, L. Chen, Z. Wu, Y. Liang, Electrochem. Solid State Lett. 2 (1999) 547.
[20] J. Yang, Y. Takeda, N. Imanishi, J.Y. Xie, O. Yamamoto, J. Power Sources 97–98 (2001) 216.
[21] J. Yang, Y. Takeda, N. Imanishi, O. Yamamoto, J. Electrochem. Soc. 146 (1999) 4009.
[22] M. Winter, J.O. Besenhard, Electrochem. Acta 45 (1999) 31.
[23] Z. Shi, M. Liu, D. Naik, J.L. Goble, J. Power Sources 92 (2001) 70.
[24] K. Nishio, N. Furukawa, in: J.O. Besenhard (Ed.), Handbook of Battery Materials, Wiley, New York, 1999, p. 19.
[25] C. Wang, A.J. Appleby, F.E. Little, J. Power Sources 93 (2001) 174.